

# SEM-EDS to probing morphological and physiological changes produced by a porphyrin photosensitizer in *Psammobatis extenta* electrocytes

María Prado<sup>(1)</sup> [inprado@criba.edu.ar](mailto:inprado@criba.edu.ar); Julio Santiago<sup>(2)</sup> [jsantiago@ipen.gob.pe](mailto:jsantiago@ipen.gob.pe)

(1) Universidad Nacional del Sur, Bahía Blanca, Argentina

(2) Instituto Peruano de Energía Nuclear, Av. Canadá 1470, Lima 1, Perú

## Resumen

The morphological and physiological changes produced by the intracellular localization of an alkyl long-chain tetraphenylporphyrin photosensitizer in *Psammobatis extenta* electrocytes were studied by means of SEM – EDS technique. The photosensitizer localizes in the electromotor nerves and the nuclear chromatin of electrocytes. Both structures exhibited intense fluorescence, whereas, the mitochondria were only slightly fluorescent. Immediately after the penetration of the photosensitizer, the electrocytes swell and the convex faces lose all their invaginations. This effect is due to the flux of chloride and sodium ions into the electrocytes, in accord to the electron-probe X-ray microanalysis.

## 1. Introduction

Photosensitizers have a wide spectrum of applications ranging from material sciences to medicinal and biological sciences. They are used in photocatalysis to improve the efficiency of semiconductors. For example, ruthenium bipyridyl complexes or phthalocyanine derivatives are used to improve the TiO<sub>2</sub> absorption range of solar energy.<sup>1</sup> In medicine, the main application of photosensitizers is in the photodynamic therapy of cancer (PDT) as well as several non-malignant conditions such as age related macular degeneration.<sup>2</sup> PDT take advantage in the high affinity of some photosensitizers (mainly porphyrin and phthalocyanine derivatives) to cancer cells and the easy way they absorb visible light to generate singlet molecular oxygen.<sup>3</sup> This specie is highly reactive and modify chemically important biomolecules, including lipids, proteins, and nucleic acids. Therefore, these biomolecules cannot accomplish their function and, consequently, the cells die.<sup>4,5</sup> In biology, photosensitizers are used to inactivate bacteria and protozoa.<sup>6,7</sup> A practical application of this knowledge may be water disinfection for human consume or the inhibition of biofilm formation.

To understand cell death in PDT or inactivation of bacteria is important to know in which part of the cell is attached the photosensitizer. In general, lipophilic photosensitizers accumulate in the membrane of a cell and its organelles.<sup>8</sup> On the other hand, hydrophilic, as well as aggregated states of photosensitizers, are localized mainly in lysosomes and endosomes.<sup>9</sup> Another important fact is to observe the morphological changes induced by the photosensitizers in cells by the chemical modifications of biomolecules.

Scanning electron microscopy (SEM) coupled with Energy Dispersive X-ray Analyzer (EDS) system was used to study the morphology (shape and size) and elemental composition of material surfaces. The use of these techniques in areas different than material sciences is increased in the last decade. The application of this technique in biology include the monitoring of calcification of human vascular cells,<sup>10</sup> and the *in vivo* tissue response of implants.<sup>11</sup> In the latter case, EDS technique demonstrated the formation of a phosphorous-rich zone in the interface between bone and the implants.<sup>11</sup> EDS technique was also used to measure the elemental concentration of monovalent cations (Na<sup>+</sup>, Cl<sup>-</sup>, and K<sup>+</sup>) during the degradation phase of apoptosis of U937 human monoblastoid cell line.<sup>12</sup>

In this work we use SEM-EDS technique to obtain additional information related to the morphological changes observed after the intracellular localization of the 5,10,15,20-tetrakis(4-*n*-dodecylphenyl)-porphyrin

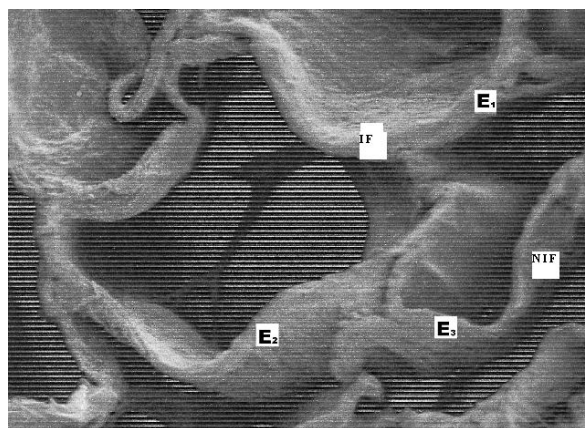


Fig.1. Scanning electron micrograph showing three electrocytes (x100).

(C<sub>12</sub>TPPH<sub>2</sub>) in *Psammobatis extenta* electrocytes. This specie belongs to the Rajidae, one of the three groups of weak electric fish. The other ones are the Gymnotiformes and the Mormyriiforms. The electric organs of *Psammobatis extenta* are constituted by macroscopic cells called electrocytes. Electrocytes are found in an alveolar arrangement on the antero-posterior axis.<sup>13,14</sup> The few organelles presented in electrocytes can be observed easily with optical microscope. The electrocytes are highly polarized and multinuclear cells. *P. extenta* electrocytes are semicircular in shape (Fig. 1) and have their concave face receiving innervation (IF) from electromotor neurons of the spinal cord. The other face, which is convex, is non-innervated (NIF) and shows a system of caveolae.<sup>15,16</sup> The nuclei are localized at the posterior region of the cytoplasm. The shape of the Rajidae electrocytes varies from cup-shaped, modified cup-shaped cells (or semicircular) to disc-shaped. The electrocyte structure reflected the phylogeny of skates. Thus the most primitive is the cup-shaped and the most derived is the disc-shaped.<sup>17</sup> The study of the *Psammobatis extenta* electrocytes is interesting because they are modified cup-shaped cells<sup>15</sup> with myoproteins and then primitives.<sup>18</sup>

## 2. Experimental Method

### Materials and chemicals

Adult *Psammobatis extenta* fish were from the Estuary of Bahía Blanca, Buenos Aires Province, and from San Antonio Oeste, Rio Negro Province, Argentine. Immediately after dissection, the electric tissue was frozen at -80°C until use.

All chemical reagents were used as purchased. Solvents were purified following the standard methods.

### Photosensitizer

C<sub>12</sub>TPPH<sub>2</sub>, a TPP derivative, was prepared in two steps (Scheme 1), following the literature procedures.<sup>19,20</sup> Briefly this involved the following:

**Synthesis of *n*-Dodecylbenzaldehyde:** *n*-dodecylbenzene and freshly distilled TiCl<sub>4</sub> were mixed in CH<sub>2</sub>Cl<sub>2</sub>. The mixture was cooled and 1,1-dichlorodimethyleter was added drop by drop, keeping the temperature below 10°C. After 45 minutes at room temperature, the mixture was extracted with CH<sub>2</sub>Cl<sub>2</sub> and the organic phase dried with anhydrous Na<sub>2</sub>SO<sub>4</sub>. *n*-dodecylbenzaldehyde was purified as an yellowish viscous oil after column chromatography (Silicagel, CHCl<sub>3</sub>/hexane 1:1). Yield 60%.

**Synthesis of C<sub>12</sub>TPPH<sub>2</sub>:** *n*-dodecylbenzaldehyde was mixed with pyrrole in propionic acid and heated at 170°C for 30 minutes. After cooling to room temperature, the solid was filtered and redissolved with CHCl<sub>3</sub>, then a solution of DDQ/benzene was added and heated for 30 minutes at 70°C. The C<sub>12</sub>TPPH<sub>2</sub> was purified by column chromatography (Al<sub>2</sub>O<sub>3</sub>, activity I, CH<sub>2</sub>Cl<sub>2</sub>) followed by recrystallization in CHCl<sub>3</sub>/acetone. Yield 15%.

The purity was controlled by <sup>1</sup>H-NMR and elemental analysis. λ<sub>max</sub> (CHCl<sub>3</sub>) = 418 nm.

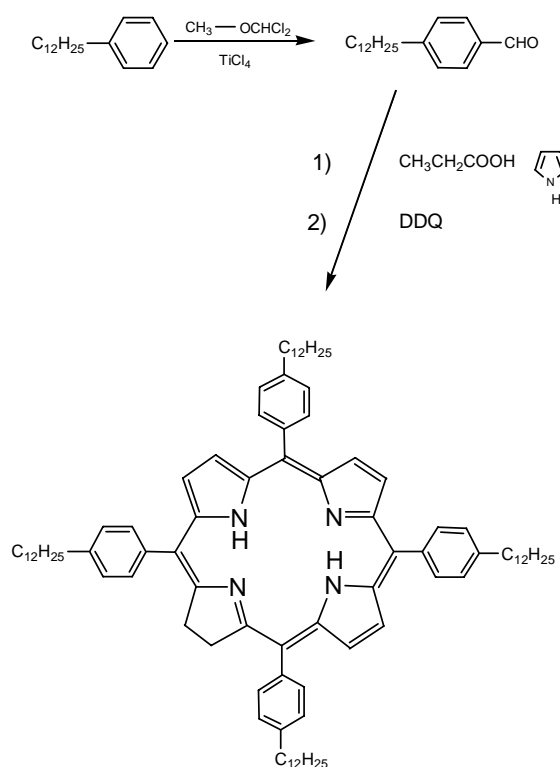
### Epifluorescence microscopy

Cryostat sections of Rajidae electric organ, about 10 μm, were treated in three different systems:

**System A:** Sections were incubated for 3 minutes with 1,2 x 10<sup>-4</sup> M solution of C<sub>12</sub>TPPH<sub>2</sub> in chloroform and were fixed for 5 min at 4°C in a mixture of 3.7% formaldehyde and 0.5% glutaraldehyde in 0.05 M phosphate buffer, pH 7.4.

**System B:** Sections were treated for 1 minute with C<sub>12</sub>TPPH<sub>2</sub> diluted in CHCl<sub>3</sub>, 1 μg/10 μL, and then in 90 μL of a mixture of 70% ethanol and 3mM imidazole buffer, pH 7,2, yielding a final concentration of 1,2 x 10<sup>-4</sup> M. Then fixed as described for system A.

**System C:** Sections were treated as in system B but xylene was used instead of chloroform and the TPP derivative concentration was 5 times higher.



**Scheme 1** Synthetic route to obtain C<sub>12</sub>TPPH<sub>2</sub>.

After fixation, sections were washed in PBS or imidazole buffer for 5 min., mounted with Citifluor and observed with an epifluorescence Nikon Optiphot microscope equipped with filter G and 580W supplementary filter. Photomicrographs were taken using a Nikon camera and ILFORD HP 35 400 ASA film. As negative control the sections were treated as described above but with omission of the TPP derivative.

### SEM-EDS experiments

For control experiments electric segments were incubated for 1 h. with glutaraldehyde 1.5 % in 0.05 M phosphate buffer pH 7.4. Then sections were washed 3x with the same buffer for 10 min. Samples were dehydrated successively with EtOH 50, 75, 90 y 100%. After solvent evaporation samples were coated with carbon in a sputter coater model 3 (Pelco, Ted Pella Inc.)<sup>18</sup>

For SEM-EDS analysis electric organ segments of 1x2 mm were treated with the TPP derivative in similar conditions described for fluorescence microscopy. After evaporation of solvents, samples were metalized with gold (200Å) in a sputter coater model 3 (Pelco, Ted Pella Inc.) and oriented for observation by a JEOL 35 Scanning Electron Microscope equipped with EDAX Si(Li) energy dispersive X-ray detector. Also it was used a Philips PSEM 500 Scanning Electron Microscope equipped with EDAX. In this case samples were coated with carbon. Microanalysis was carried out at the non-innervated face of the electrocytes, because it shows invaginations and the photosensitizer is concentrated on this kind of tissue.

All the EDS spectra showed in this paper are Relative Intensity (arbitrary units) vs Energy (keV).

## 3. Results

### Epifluorescence microscopy

In contrast with the negative control the intracellular localization of the photosensitizer were observed easily by fluorescence microscopy and phase contrast microscopy. The fluorescence micrograph (Fig. 2) shows part of two electrocytes treated with system A. It can be observed strong fluorescence in nuclei but very slight in mitochondria. Additionally the photosensitizer shows affinity for the terminal nerves, the synaptic region. The same was observed with the phase-contrast micrograph of sections treated with systems B and C.<sup>21</sup>

### SEM-EDS experiments

SEM-EDS experiment was performed on the tissue sections without any treatment with solvents or photosensitizer (Fig. 3). This micrograph of non-innervated face shows a

system of caveolae. The relative semi-quantitative weight % ( $K_{\alpha}$ ) for oxygen was 70%.  $\text{Cu}^{2+}$  and  $\text{Zn}^{2+}$  are present in low concentration.

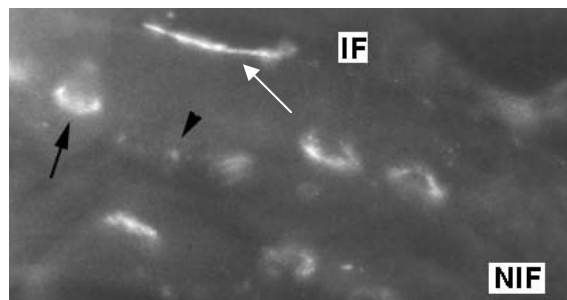


**Fig. 2.** Localization of  $\text{C}_{12}\text{TPPH}_2$  in the nuclei (black arrow), terminal nerves (white arrow) and in mitochondria (arrow head) of an electrocyte (x600).

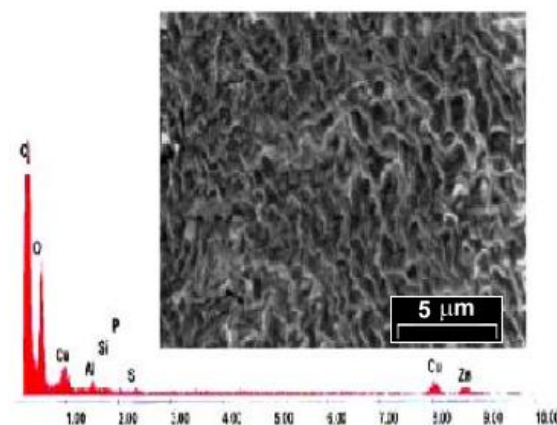


**Fig. 3.** EDS spectrum and scanning electron micrograph (x2000) of non-innervated face of an electrocyte before any treatment.

After treatment of the electrocyte, from Bahía Blanca, with  $\text{C}_{12}\text{TPPH}_2$  in chloroform, system A, (fig. 4), the relative semi-quantitative weight % ( $K_{\alpha}$ ) for oxygen, sodium and chloride ions were: 39, 17 and 15, respectively. Compared to negative controls, the peak for  $\text{Na}^+$  is 5-fold larger and for oxygen the variation is not significant. Also, the peaks of  $\text{Ca}^{2+}$  and  $\text{K}^+$  are presents but are very small. Immediately after the penetration of the TPP derivative ( $1,2 \times 10^{-7}$  M in chloroform) in the electrocytes, they start to swell and the convex face loses all their invaginations (Fig. 4b).

Electrocytes, from San Antonio, treated with systems B and C show similar behavior than in  $\text{CHCl}_3$ . In both cases the EDS spectra show a new peak corresponding to chloride anion (Fig. 5). The semi-quantitative weight % ( $K_{\alpha}$ ) for this element was 47% (system B) and 33% (system C), in spite of the higher concentration of  $\text{C}_{12}\text{TPPH}_2$  in system C (5-fold higher). Other elements were also detected: Si (19%) and  $\text{K}^+$  (28%) in system B; while slightly different ratios were observed in

system C, Si (32%) and K<sup>+</sup> (25%). Na<sup>+</sup> were observed in very low concentration, 6 % and 10 % respectively.

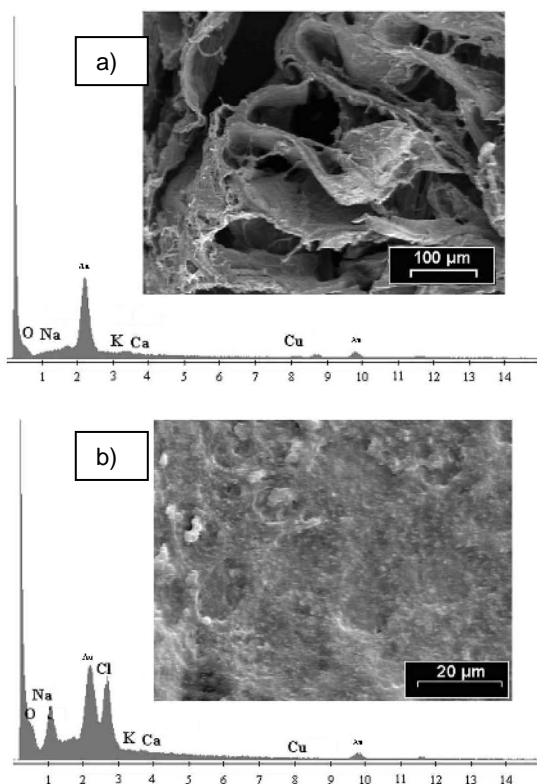


**Fig. 4.** EDS spectra and scanning electron micrographs of non-innervated face of an electrocyte after treatment with a)  $\text{CHCl}_3$ , and b)  $\text{C}_{12}\text{TPPH}_2$  in  $\text{CHCl}_3$ .

## 4. Discussion

### Photosensitizer

The synthesis of the  $\text{C}_{12}\text{TPPH}_2$  was performed following the literature methods with slight changes. We avoid the use of benzene (because of its toxicity) when it was possible. The low overall yield is normal for this kind of porphyrins. This compound was already studied in regard to its thermal properties. It was found to exhibit two discotic lamellar phases. The phases change and the transition temperatures are: C - 31°C - D<sub>L</sub> - 52°C - D<sub>L</sub>' - 155°C - Isotropic.<sup>20</sup> However, their lyotropic liquid crystal properties are not yet studied.

This TPP derivative is very soluble in apolar solvents like  $\text{CHCl}_3$ . To use polar solvent we have to include imidazol buffer in the system to avoid precipitation.

### Epifluorescence microscopy

The intracellular localization was monitoring easily by the observation of the red fluorescence exhibited by the  $\text{C}_{12}\text{TPPH}_2$ . The organic compound distributes uniformly over

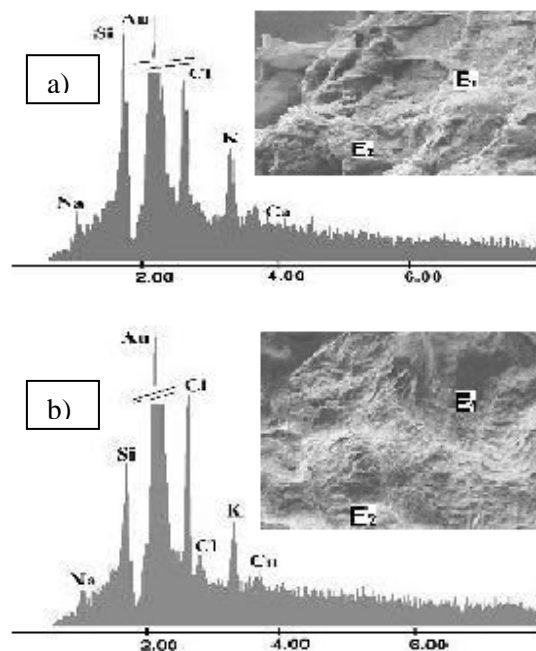


**Fig. 5** EDS spectra and scanning electron micrographs (x80) of the electric organ segments treated with the TPP derivative in a) chloroform-EtOH-imidazole buffer, and b) xylene-EtOH-imidazol buffer.

the terminal nerves around the electrocytes, and specially in nuclei. The affinity of this lipophilic photosensitizer for the nerves is explained because this tissue is rich in fatty acids. Surprisingly, this compound does not exhibit affinity for the entire membrane cell. The nuclei show an intense red fluorescence and the shape of this fluorescence were similar to the semicircular distribution of the chromatin of these cells (Fig. 2), suggesting that the TPP derivative interacts with DNA. In contrast, the mitochondria show slight fluorescence. This localization is unusual for a photosensitizer of similar polarity. For example, a lipophilic phthalocyanine localizes on the lysosomes.

In the conditions of our experiments, the chloroform does not seem to provoke visible damage to membrane cells. Fig. 2 shows that membrane cells keep their integrity.

The intracellular localization is not solvent-dependent. The same distribution was observed with system C but the resolution of the fluorescence micrographs are better in chloroform than in xylene-EtOH-imidazol buffer system. This may be due to a better solubility of the  $\text{C}_{12}\text{TPPH}_2$  in  $\text{CHCl}_3$ .<sup>21</sup>

### SEM – EDS

Initially EDS measurements were performed on sections coated with carbon in order to check there are no metal peaks in the region where gold peak appears. Energy dispersive spectrum shows a high peak for oxygen in the original cell without any treatment (Fig. 3). This may be related to generation of

oxygen and oxidative stress in the electrocyte.  $Zn^{++}$  and  $Cu^{++}$  cations are also present in the electrocytes, these cations have antioxidant effect and are probably including with the superoxide dismutase enzyme.<sup>22</sup> This oxygen peak was not observed anymore in the EDS analysis of sections treated with solvents (systems A-C) alone or with the TPP derivative (Fig. 4, 5). It is surprising that there is no peaks for common cations as  $Na^+$ ,  $K^+$  and  $Ca^{2+}$  in *Psammobatis extenta* electrocytes.

There are several reports on chloroform cytotoxicity. For example, cytolethality on rat hepatocyte was induced after 3 h incubation in chloroform.<sup>23</sup> However the effect of chloroform alone seems to be not very important in the conditions of our experiments, 5 minutes incubation. The morphology of electrocytes is similar before and after treatment with chloroform (Fig. 1 and 4a). However their EDS spectra are different. The EDS spectrum of Fig. 4a compared to Fig. 3 indicates that the semi-quantitative weight (%) for oxygen decreases to the half after treatment with chloroform but new small peaks of  $Na^+$ ,  $K^+$  and  $Ca^{2+}$  could be observed. The signal of Al, Si and P observed in normal electrocytes are not observed after the treatment with chloroform. Maybe they are covered by other signals. Completely different effect can be observed after the electrocytes incubation in a TPP derivative in chloroform solution. The penetration of the photosensitizer in electrocytes provokes a dramatic increasing of  $Na^+$  concentration and the appearance of a new big peak corresponding to  $Cl^-$  anion. As a consequence of this influx of ions the electrocytes swelling (Fig. 4b). The reason of the ions flux inside the cell may be due to the morphological modification of cell membrane. Also conformational changes of the proteins involved in ionic channels are possible due to the presence of the photosensitizer in the terminal nerves. Because its lipophilic character, the TPP derivative have affinity of the lipophilic region of cell membranes and may interact with the proteins of ionic channels activating them.

EDS data give a good evidence for the cationic channel activation as a consequence of the porphyrin derivative fixation in cell.  $Cl^-$  influx is also observed after electrocytes treatment with TPP derivative in systems B and C as solvent (Fig. 5a and 5b). But instead of  $Na^+$ ,  $K^+$  influx is observed when  $CHCl_3$ -EtOH-imidazol buffer and xylene-EtOH-imidazole buffer used as solvent (Fig. 5a y 5b), indicating that solvents play a crucial rol in ion flux. An explanation could be that the TPP derivative are fixed in the cell membrane in different concentration and interacts with some part of the lipophilic region of some ions channel, depending its concentration, and changing its behaviour. Also we can consider that even in the experimental conditons small amount of singlet oxygen could be generated and

modify the membrane properties allowing the influx of chloride anion.<sup>24</sup> The possible changes in membrane include current, potential, ionic gradients, action potential duration and amplitude, after depolarization, spontaneous activity and loss of excitability.<sup>25,26</sup> It should be pointed out that chloride channel activation is not usual for weakly electric fish like *Psammobatis extenta*. However, the presence of a voltage-gated chloride channel was demonstrated in the non-innervated plasma membrane of *Torpedo* electrocyte, a strongly electric fish.<sup>27</sup> It should be noted that  $K^+$  and  $Cl^-$  concentrations play an important role in apoptosis mechanism. Targeting of  $K^+$  channels was proposed as a potential therapeutic tool in modulating apoptosis to maintain the balance between cell proliferation and cell death that is essential to the normal development and function of an organism.<sup>28</sup>

Another interesting fact is the increasing of the silicon peak. The semi-quantitative weight (%) for this element increase from 13 % in electrocytes without any treatment to 19 % (system B) and 32 % (system C). The latter is a normal amount considering that system C was 5x more concentrating than B.

## 5. Conclusions

These results constitute a suggestive evidence for chloride channel activation as a consequence of the penetration of  $C_{12}TPPH_2$  in electrocytes. The massive intracellular accumulation of  $Cl^-$  and specially the influx of  $Na^+$  lead to cell swelling, and the subsequently necrotic response of cells. The activation of chloride channel by this TPP derivative may constitute an alternative in the treatment of the cystic fibrosis, which is related to a dysfunction of the chloride ion transport.

In contrast, the increase of  $Ca^{2+}$  concentration in electrocytes suggests a participation of an apoptotic mechanism. Moreover, the interaction of  $C_{12}TPPH_2$  with DNA, and even the low amount of mitochondrial-bound porphyrin, may contribute to cell death by apoptotic mechanism after excitation with light.

SEM-EDS is a powerfull technique to obtain information that allow to explain the morphological and physiological changes and elemental composition variations after the treatment of cells with photosensitizers during the photodynamic therapy of cancer.

## References

- 1 A. Nogueira, A. Formiga, H. Winnischofer, M. Nakamura, F. Engelmann, K. Araki and H. Toma, *Photochem. Photobiol. Sci.* **3** (2004) 56.

- 2 H. van den Bergh, *Semin. Ophthalmol.* **16** (2001) 181.
- 3 M. Fournier, C.Pépin, D. Houde, R. Ouellet and J. van Lier, *Photochem. Photobiol. Sci.* **3** (2004) 120.
- 4 M. Davies, *Photochem. Photobiol. Sci.*, **3** (2004) 17.
- 5 N. L. Oleinick, R. L. Morris and I. Belichenko, *Photochem. Photobiol. Sci.* **1** (2002) 1.
- 6 E. Reddi, M. Ceccon, G. Valduga, G. Jori, J. Bommer, F. Elisei, L. Latterini and U. Mazzucato, *Photochem. Photobiol.* **75** (2002) 462.
- 7 Z. Malik, T. Babushkin, S. Sher, J. Hanania, H. Ladan, Y. Nitzan and S. Salzberg, *Int. J. Biochem.* **25** (1993) 1399.
- 8 A. Graham, G. Li, Y. Chen, J. Morgan, A. Oseroff, T. Dougherty and R. Pandey, *Photochem. Photobiol.* **77** (2003) 561.
- 9 K. Berg and J. Moan, *Photochem. Photobiol.* **65** (1997) 403.
- 10 D. Proudfoot, J. Skepper, C. Shanahan and P. Weissberg, *Arterioscler. Thromb. Vasc. Biol.* **18** (1998) 379.
- 11 H. Liao, H. Mutvei, M. Sjostrom, L. Hammarstrom and J. Li, *Biomat.* **21** (2000) 457.
- 12 S. Zabiti, F. Arrebola, F. Cañizares, M. Cubero, E. Fernandez-Segura, P. Crespo and A. Campos, *Int. J. Dev. Biol.*, **45(S1)** (2001) S163.
- 13 M. Bennett, *Encyclopedia of Neuroscience*, G. Adelman, Birkhauser (Ed.), 1987, **1**, 365.
- 14 G. Fox, M. Kriebel and G. Pappas, *Anat. Embryol.*, **181** (1990) 305.
- 15 M. Prado Figueroa, M. Vidal and A. Barrantes, *Biocell*, **19** (1995) 113.
- 16 M. Prado Figueroa, F. Barrera and G. Schmidt, *Archivos de la Memoria de la ciudad de bahía Blanca*, EdiUNS, **3** (2003) 121.
- 17 J. C. Ewart, *Phil. Trans. Roy. Soc. London* **183B** (1892) 378.
- 18 A. Vidal, M. Prado Figueroa, M.E. Eberwein, E. Kreda and F.J. Barrantes, *Comp. Biochem. Physiol.* **116A** (1997), 113-118.
- 19 Y. Shimizu, M. Miya, A. Nagata, K. Ohta, A. Matsumura, I. Yamamoto and S. Kusabayashi, *Chem. Lett.* 1991, 25.
- 20 Y. Shimizu, M. Miya, A. Nagata, K. Ohta, I. Yamamoto and S. Kusabayashi, *Liq. Cryst.* **14** (1993) 795.
- 21 M. Prado Figueroa, J. Santiago, *Photochem. Photobiol. Sci.*, **3** (2004) 33.
- 22 M. Prado Figueroa, IX Congreso Ibero-Americano de Biología Celular, Campinas, Brasil, 2004.
- 23 P. Ammann, C. Laethem, G. Kedderis, *Toxicol. Appl. Pharmacol.*, **149** (1998) 217.
- 24 Joseph I. Kourie, *Am. J. Physiol. Cell Physiol.*, **275** (1998) C1.
- 25 Elliott, S. J., and W. P. Schilling, *Am. J. Physiol. Heart Circ. Physiol.* **163** (1992) H96.
- 26 R. Jabr, W. Cole, *Circulation Research.* **76** (1995) 812.
- 27 M. White and C. Miller, *J. Gen. Physiol.*, **78** (1981) 1.
- 28 Remillard and J. Yuan, *Am. J. Physiol. Lung Cell Mol. Physiol.*, **286** (2004) L49.